Obrabotka metallov (tekhnologiya, oborudovanie, instrumenty) = Metal Working and Material Science. 2025 vol. 27 no. 1 pp. 172–191
ISSN: 1994-6309 (print) / 2541-819X (online)
DOI: 10.17212/1994-6309-2025-27.1-172-191

NSTU NETI

Obrabotka metallov - Metal Working and Material Science

Journal homepage: http://journals.nstu.ru/obrabotka_metallov

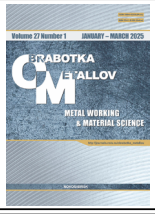

DLP 3D printing and characterization of PEEK-acrylate composite biomaterials for hip-joint implants

Yogiraj Dama [1, a, *], *Bhagwan Jogi* [1, b], *Raju Pawade* [1, c], *Shibam Pal* [2, d], *Yogesh Gaikwad* [2, e]

[1] Dr. Babasaheb Ambedkar Technological University, Lonere, Raigad, Maharashtra, 402103, India
[2] CSIR-National Chemical Laboratory, Pashan Pune, Maharashtra, 411008, India

[a] https://orcid.org/0009-0008-5404-4347, yogirajdama@dbatu.ac.in; [b] https://orcid.org/0000-0003-2099-7533, bfjogi@dbatu.ac.in;
[c] https://orcid.org/0000-0001-7239-625X, rspawade@dbatu.ac.in; [d] https://orcid.org/0000-0002-3681-5039, shibampal123456@gmail.com;
[e] https://orcid.org/0009-0003-3211-0861, ym.gaikwad@ncl.res.in

ARTICLE INFO

Article history:
Received: 26 November 2024
Revised: 14 December 2024
Accepted: 06 January 2025
Available online: 15 March 2025

Keywords:
3D Printing
Biomaterials
FDM
Implant
Print orientation
PLA
Wear behavior

ABSTRACT

Introduction. Hip joint replacement is considered the most complex and critically important orthopedic surgical procedure compared to knee and shoulder joint replacements. Over the past few decades, there has been significant advancement in hip joint replacement technology, and various biomaterials have been substantially improved. An increasing number of hip joint replacement surgeries are now successful, assisting individuals in regaining normal daily activity and work capacity comparable to their pre-fracture state. However, the need for revision surgery, specifically for implant replacement, is still observed in active patients several years following the initial operation. This underscores the need to develop durable biomaterials and customized hip joint implants to reduce implant wear and the risk of dislocation. This research study explores a novel *PEEK*-in-acrylate composite biomaterial with varied weight percentages of *PEEK* (0 %, 5 %, and 10 %) in an acrylate-based matrix. Tests were conducted to determine its properties, biocompatibility, and 3D printability. Based on the developed material, pins (in accordance with the *ASTM* standard) were fabricated using 3D printing for subsequent wear rate studies. The potential use of the developed composite materials for hip-joint applications was also thoroughly investigated. **The purpose of this study** is to develop and investigate a new *PEEK* in Acrylate composite biomaterial with varied weight percentages of *PEEK* (0 %, 5 %, and 10 %) in an acrylate-based matrix. The research includes an assessment of the material's properties, biocompatibility, and 3D printability. Using digital light processing (*DLP*) 3D printing technology at room temperature, pins (in accordance with the *ASTM* standard) were fabricated. An experimental study of dry sliding wear resistance was conducted on the resulting samples to determine the effect of *PEEK* weight fraction on the wear rate and frictional performance against an SS 316 steel disk. Scanning electron microscopy (*SEM*) and Energy-dispersive X-ray spectroscopy (EDS) were used to analyze the surface structure and element distribution within the material. **The Methods of Investigation.** Digital Light Processing (*DLP*) 3D Printing technique was used to 3D Print the *ASTM* pins and Acetabular liner with different weight fraction of *PEEK* in acrylate. Dry sliding wear tests were carried out using a pin-on-disk tribometer. During testing, the disk rotation speed and the normal load on the pin were varied. The studies were designed to determine the influence of input parameters on the wear rate. A total of nine experiments were conducted for each *PEEK* weight fraction, with a sliding distance of 4 km per experiment. The load ranged from 20 to 100 N, and the sliding speed varied from 450 to 750 rpm. Surface structure and element distribution were analyzed by Energy-dispersive X-ray spectroscopy (*EDS*) and Scanning electron microscopy (*SEM*). **Result and Discussion.** Current study demonstrates the advantages of varying the weight fraction of PEEK in Acrylate for *DLP*-fabricated biomaterials. Analysis of the *SEM*, *EDS*, and wear testing results indicated that the composite with 10 wt % *PEEK* in Acrylate exhibited superior microstructural integrity, elemental homogeneity, and significantly improved wear resistance. The 10 wt % *PEEK* in Acrylate composite, fabricated via *DLP* 3D printing, is suitable for biomedical implant and healthcare applications

For citation: Dama Y.B., Jogi B.F., Pawade R., Pal S., Gaikwad Y.M. DLP 3D printing and characterization of PEEK-acrylate composite biomaterials for hip-joint implants. *Obrabotka metallov (tekhnologiya, oborudovanie, instrumenty) = Metal Working and Material Science*, 2025, vol. 27, no. 1, pp. 172–191. DOI: 10.17212/1994-6309-2025-27.1-172-191. (In Russian).

Introduction

Hip joint implants play a key role in contemporary orthopedic surgery and are extensively used for the treatment of conditions such as osteoarthritis, rheumatoid arthritis, hip fractures, and congenital deformities [1]. These implants are designed to replace damaged hip joints, restore locomotor function, and reduce pain [2]. Due to their critical function in supporting body weight and enabling movement, materials for

*** Corresponding author**
Jogi Bhagwan Fatru, Professor
Dr. Babasaheb Ambedkar Technological University,
Lonere, Raigad,
402103, Maharashtra, India
Tel.: +91 942-116-6370, **e-mail:** bfjogi@dbatu.ac.in

hip implants must possess superior mechanical properties, biocompatibility, and durability [3]. Additive Manufacturing (*AM*), or 3D printing, has fundamentally transformed biomedical engineering by enabling the creation of complex geometries and personalized implants tailored to individual patient anatomy [4]. In particular, additive manufacturing techniques facilitate the use of porous titanium alloys, which promotes improved osseointegration and minimizes stiffness mismatch between the implant and bone, thereby ensuring favorable long-term patient outcomes [5]. The present study evaluates the mechanical properties, biocompatibility, and overall effectiveness of hip joint implants fabricated from both traditional materials and using additive manufacturing technologies [6]. The aim of this work is to investigate the potential of additive manufacturing to improve patient outcomes by overcoming the limitations inherent in conventional implants, such as stress shielding and insufficient bone integration [7].

Among the wide range of polymer biomaterials, polyetheretherketone (*PEEK*) stands out due to its suitability for 3D printing, surpassing other materials used in orthopedic implantology [8]. *PEEK* is employed in conventional manufacturing processes to develop various biomedical implants [9]. It is characterized by high strength and a *Young's* modulus closely matching that of human bone, which minimizes stress shielding and enhances implant stability. Due to these properties, *PEEK* is a promising material for the fabrication of load-bearing components, such as hip joint cups [10]. *PEEK* possesses high thermal stability, with a melting point of approximately 343 °C. This allows it to withstand sterilization processes required for medical implants without degradation, ensuring the retention of its properties throughout its lifespan within the human body [11]. Furthermore, *PEEK* exhibits exceptional chemical resistance to a variety of chemical substances, including solvents, acids, and bases, ensuring its durability and long-term stability in the physiological environment without eliciting adverse reactions [12]. The biocompatibility of *PEEK* as a reliable material for biomedical applications has been validated by numerous studies [13–14].

For an adequate assessment of *PEEK*'s applicability in load-bearing orthopedic implants, mechanical testing and wear resistance studies are of paramount importance. Specifically, *Reddy* et al. [15] investigated the mechanical properties of 3D-printed *PEEK* specimens intended for dental implants and found that specimens printed with a (45°/−45°) raster angle exhibited improved tensile, compressive, and flexural strength. This indicates the potential of *PEEK* as an alternative to titanium and zirconia for dental applications. In their studies of a *PEEK-*Ti_6Al_4V composite implant, *Zhang* et al. [16] assessed compressive strength and wear resistance via mechanical testing, in accordance with standard *ASTM* testing protocols. *Du* et al. [17] investigated the mechanical characteristics of scaffolds made from the *PEEK-SiN* composite material.

Scanning electron microscopy (*SEM*) analysis of *PEEK* implants provides valuable insights into the surface morphology and microstructural features of the material. For example, *Lim* et al. in 2019 [18] utilized *SEM* analysis to evaluate the porosity of various 3D-printed *PEEK* and titanium structures. The results indicated that a pore size of approximately 1.2 mm most closely matches the structure of human trabecular bone. This optimal pore size has been proven to enhance osseointegration, as *SEM* images demonstrate that the rough surface texture of porous structures promotes increased pull-out strength and, overall, improved bone integration capability [19]. Conversely, *SEM* analysis conducted by *Carpenter* et al. in 2018 [20] revealed significant differences between porous *PEEK* and porous titanium implants. In 2020, *Virpe* et al. [21] performed an analysis of polymer composites, demonstrating the successful incorporation of carbon fillers into a *PLA* matrix using *FDM* 3D-printing.

At the same time, the correlation between microstructural characteristics, as determined by *SEM*, and their influence on wear mechanisms in pin-on-disc testing remains inadequately understood [22–23]. It is noted that not all polymer biomaterials, such as *UHMWPE*, *HDPE*, and *PE*, are readily amenable to 3D printing. This necessitates the use of alternative polymers, including *PEEK*, *PLA*, and composite polymer biomaterials that are suitable for 3D-printing and meet the requirements for implants [24]. Therefore, investigating the wear rate characteristics of hip joint implants is an important task, leading to further research on wear parameters using various polymer biomaterials, composites, and coated biomaterials [25]. Various testing methods employed for evaluating the wear resistance and mechanical properties of polymer materials are useful for biomaterials as well [27–28].

The purpose of this research is to study a *PEEK* in Acrylate polymer-based biomaterial for hip-joint implant applications, which is 3D-printable at room temperature [26]. The study aims to determine the impact of reinforcement levels on microstructural integrity, elemental distribution, and wear performance, thereby aiding in the development of *PEEK*-based materials for orthopedic applications. Specifically, 3D-printed *ASTM* pins will be tested via pin-on-disc methodology to evaluate wear rate performance suitable for the long-term sustainability of implants.

Digital light processing (*DLP*) 3D-printing was conducted at the National Chemical Laboratory (*NCL*), Pune, Maharashtra, India. Wear testing was performed using equipment available at the Mechanical Engineering Department of VIIT, Pune, Maharashtra, India.

Methods

Material Preparation

Composite material formulations included 0 wt. %, 5 wt. %, and 10 wt. % *PEEK* in an Acrylate-based matrix. The composite resins were prepared by mixing the *PEEK* with the Acrylate resin at varying PEEK concentrations (5 wt. % and 10 wt. %). Fig. 1 illustrates the process flow for preparing the resin for 3D-printing and subsequently fabricating physical objects via 3D-printing. The resin pre-processing involved dissolving reactive diluents, such as Tricyclo[5.2.1.0^{2-6}]decane dimethanol diacrylate (*TCDDA*), Ethoxylated bisphenol A dimethacrylate (*BPAEDMA*), and photoinitiators, in the resin binder.

The resulting resin mixture was then loaded into a *DLP* 3D-printer, where the printing process was initiated through layer-by-layer curing of the material.

In Digital light processing (*DLP*) 3D-printing, as depicted in Fig. 2, *a*, a digital projector is used to project an image of the entire layer of the object being printed onto the surface of a vat containing liquid photopolymer resin. Upon exposure to the projected image, selective solidification of the photopolymer resin occurs, conforming to the shape of the layer. After each layer is cured, the build platform is raised, separating the formed layer from the resin vat, and a volumetric 3D model of the object is built. A washing and post-curing machine is used to clean the resulting part and to achieve final polymerization of the resin (Fig. 2, *b*). The *PEEK* in Acrylate composite biomaterial was used to 3D-print *ASTM*-compliant pins and a final liner implant.

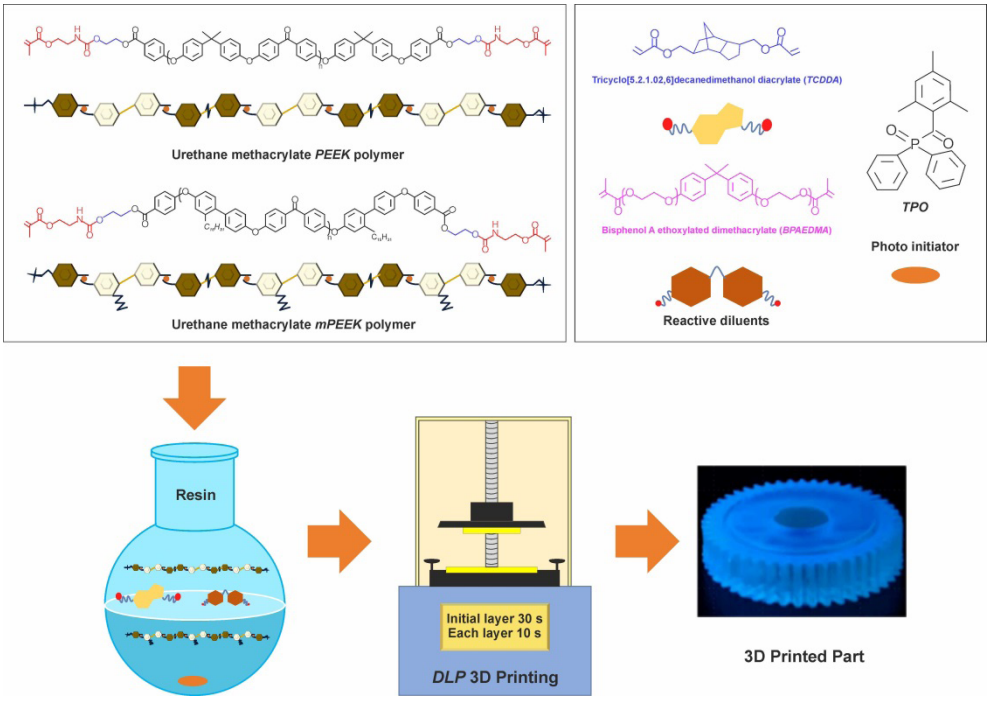

Fig. 1. Material preparation methodology used in the study [26]

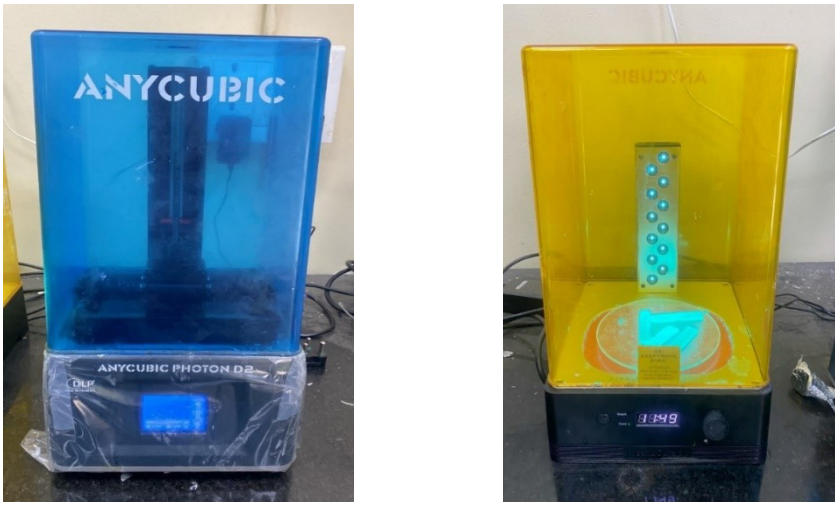

a *b*

Fig. 2. DLP 3D Printing method: *DLP* 3DPrint (*a*), Wash and Cure Machine (*b*)

The initial layer curing time was 30 seconds, followed by 10 seconds for each subsequent layer. *ASTM*-compliant pins (10 mm diameter and 15 mm height) were printed under controlled conditions to ensure uniform size and shape.

Scanning electron microscopy (SEM)

To enhance the electrical conductivity of non-metallic samples, a thin layer of gold (*Au*) was applied to the surface using a sputtering method. The gold layer, approximately 10 nm thick, was deposited using an ion sputtering device. This step is necessary to minimize charging effects that can occur during *SEM* analysis, which can lead to image distortions and reduced resolution. Gold was selected due to its high electrical conductivity and minimal interaction with the electron beam. The operating principle of the *Zeus SEM* instrument is illustrated in Fig. 3. *SEM* analysis was performed using a *Zeus* field-emission scanning electron microscope, which is characterized by high resolution and versatility in materials science. The microscope's operating accelerating voltage was 20 kV. This voltage value was chosen as an optimal compromise between the need for high-resolution imaging and ensuring sufficient penetration depth of the electron beam into the sample material. The use of lower voltages may be insufficient for penetration,

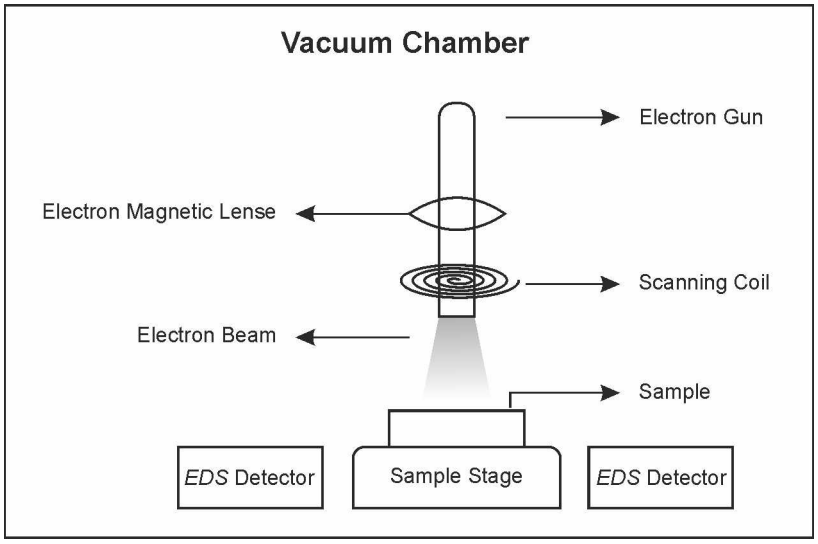

Fig. 3. Working principle of scanning electron microscope (*SEM*)

particularly in the case of composite materials with non-uniform density distribution, which would limit the analysis depth. A schematic of the experimental setup used for *SEM* analysis is shown in Fig. 3.

Sample images were acquired at various magnifications: 500×, 1,000×, 2,000×, and 5,000×. Lower magnifications were utilized to examine the overall surface morphology and to identify macroscopic defects, such as cracks, pores, and the distribution of reinforcing particles. Higher magnifications were employed to analyze microstructural details, including the interfacial boundary between the *PEEK* matrix and reinforcing particles, the morphology of individual particles, and micro-defects (micro-cracks, pores) that could negatively affect the mechanical properties of the material.

In this study, energy dispersive spectroscopy (*EDS*) and scanning electron microscopy (*SEM*) were employed to investigate the microstructural features, surface morphology, and elemental composition of the materials under investigation: pure acrylate (base material), a composite with 5 wt. % *PEEK* in Acrylate, and a composite with 10 wt. % *PEEK* in Acrylate [28]. These methods are essential for understanding the distribution of *PEEK* reinforcing particles within Acrylate matrix and for identifying potential microstructural defects that may influence the material's performance in biomedical applications.

Sample preparation for *SEM* analysis is crucial to obtain high-quality images and reliable data. Samples were sectioned into small fragments of ~10×10 mm to ensure proper accommodation within the SEM chamber. These sections were then subjected to sequential polishing, initially ground with silicon carbide paper of varying grit sizes (from 320 grit for coarse material removal to 1,200 grit for fine polishing). After achieving a smooth surface, diamond paste (3 μm, followed by 1 μm) was used to create a mirror-like finish. This final polishing step is critically important as it reduces surface roughness, which minimizes artifacts during *SEM* imaging.

Energy dispersive spectroscopy (EDS)

For detailed elemental analysis of the samples in conjunction with *SEM*, the energy dispersive X-ray spectroscopy (*EDS*) method was employed. The *EDS* method is based on the identification of characteristic X-ray radiation emitted by the sample when it is bombarded with an electron beam from a scanning electron microscope (*SEM*). The energy of these X-rays is specific to each element present in the sample, enabling their identification and quantification. For a comprehensive assessment of the material composition, *EDS* analysis was performed in multiple regions of each sample. In particular, point analysis was used to determine the elemental composition in selected local areas, primarily within the reinforcing particles and the *PEEK* matrix. A schematic of the *EDS* Instrument is shown in Fig. 4.

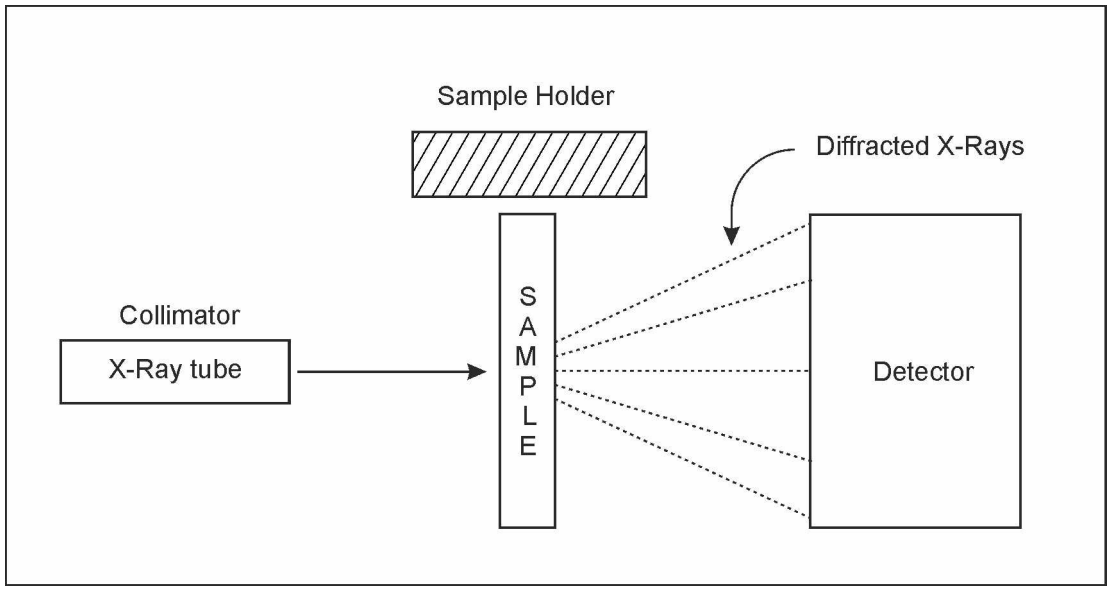

Fig. 4. Schematic representation of working principle of *EDS* instrument

Furthermore, elemental mapping was performed on larger areas to visualize the distribution of elements across the sample. This technique proved particularly useful for evaluating the uniformity of reinforcing particle distribution within the *PEEK* matrix. Analysis of the *EDS* spectra provided important data on the presence of carbon (*C*) and oxygen (*O*) as the primary elements of *PEEK*, as well as other elements introduced by the reinforcing particles. The homogeneity of the composites was assessed by comparing the elemental distribution in various analyzed regions. Significant deviations in the elemental composition indicated segregation or clustering of the reinforcing particles, which can influence the mechanical properties of the composite materials. The summary of SEM and EDS conditions is tabulated in Table 1.

Table 1

Summary of *SEM* and *EDS* Conditions

Parameter	Value
Accelerating Voltage	20 kV
Magnification Range	500×, 1000×, 2000×, 5000×
Coating Material	Gold (*Au*), ~10 nm thickness
EDS Analysis	Elemental mapping and point analysis

Pin-on-Disk wear testing

To evaluate the wear resistance of polyetheretherketone (*PEEK*) materials, including base Acrylate material, Acrylate composites with 5 wt. % *PEEK*, and Acrylate composites with 10 wt. % *PEEK*, a pin-on-disk wear test was performed. Test specimens were cylindrical pins machined from each type of material, with dimensions of 8 mm in diameter and 40 mm in height. To ensure smooth and uniform contact with the disk during testing, the pin surfaces were polished using silicon carbide abrasive paper followed by diamond paste. The wear tests were conducted on a tribometer configured in a pin-on-disk arrangement. A schematic of the test setup is shown in Fig. 5 and includes a dead weight for applying a constant load to the pin, a motor for rotating the disk, and a counterbody (*SS 316* stainless steel) in the form of a disk with a surface roughness of 0.1 μm to provide a controlled and consistent contact surface.

To ensure reproducibility of results and maintain uniform testing conditions, all experimental parameters were standardized. A normal load of 10 N was applied to each pin using dead weights. The disk was rotated at a constant sliding speed of 1 m/s to simulate wear conditions representative of orthopedic implants. The duration of each test corresponded to a total sliding distance of 1,000 m, to ensure that sufficient wear data

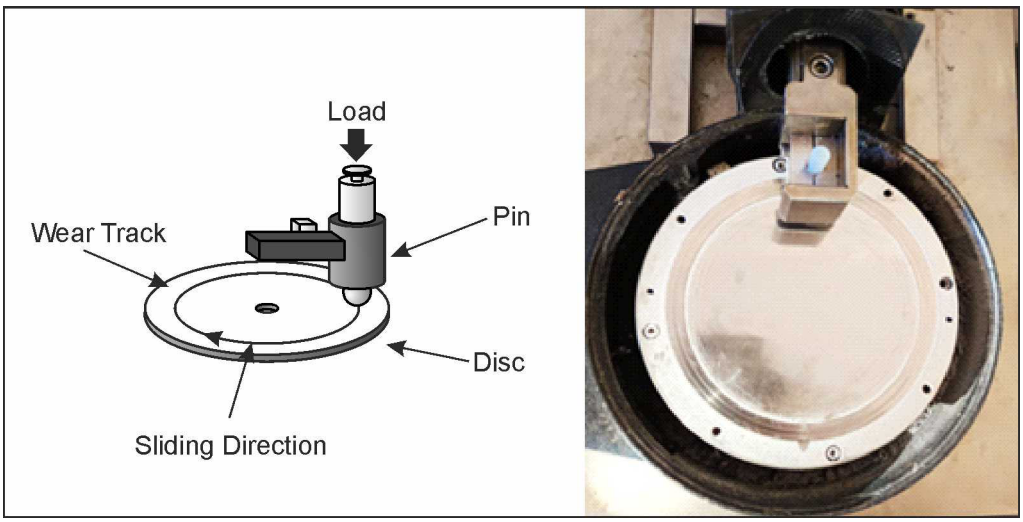

Fig. 5. Experimental test set up used for wear testing study

was collected. The tribometer was pre-calibrated to ensure high accuracy in maintaining the applied load, sliding speed, and disk rotation speed. During the test, the vertically mounted pins exerted constant pressure against the rotating stainless steel disk, inducing wear as a result of sliding contact.

After completion of the tests, the worn surfaces of the pins were analyzed using scanning electron microscopy (*SEM*) to investigate the wear mechanisms and surface degradation patterns of each *PEEK* composite material. Particular attention was given to the surface morphology to establish a relationship between reinforcement level and wear performance. The key parameters of the pin-on-disk wear tests (materials, load, speed, and sliding distance) are summarized in Table 2.

Table 2

Summary of Pin-on-Disk Testing Conditions

Parameter	Value
Pin Material	5 % wt. *PEEK* in Acrylate, 10 % wt. *PEEK* in Acrylate
Disk Material	*SS 316*
Normal Load	10 N
Sliding Speed	1 m/s
Sliding Distance	1,000

Results and Discussion

A 3D-printed *PEEK* in Acrylate composite biomaterial was thoroughly examined for its suitability in hip hip-joint applications. As part of this research, a novel biomaterial — a *PEEK* in Acrylate composite — was developed, incorporating varying *PEEK* content (0 wt. %, 5 wt. %, and 10 wt. %) in Acrylate base material. Tests were conducted to determine the material properties, biocompatibility, and 3D-printability. *ASTM* standard pins were fabricated using digital light processing (*DLP*) 3D-printing at room temperature. An experimental study of wear under dry sliding friction conditions was performed on the *PEEK* composites with varying percentage concentrations within the Acrylate. An SS 316 steel disk was used as the counterbody. The objective of the tests was to assess the effect of *PEEK* content on the wear resistance and wear rate. Scanning electron microscopy (*SEM*) and energy dispersive X-ray spectroscopy (*EDS*) techniques were employed to analyze the surface structure and elemental composition of the materials. The results and conclusions obtained from the *SEM* and *EDS* analyses and the wear tests are presented below.

Characterization of the base acrylate material

Surface morphology and microstructural features

The base Acrylate material was investigated using scanning electron microscopy (*SEM*) at magnifications ranging from 500× to 5,000× (see Fig. 6, *a*, *b*, and *c*) with an accelerating voltage of 20 kV. Imaging settings were selected for detailed analysis of the surface structure and microscopic characteristics of the material, enabling the identification of both large-scale and small-scale features. *SEM* images acquired at 500× magnification revealed a predominantly smooth surface small ripples evenly distributed throughout the material. The smooth surface morphology of this polymer indicates a high-quality manufacturing process and the absence of macroscopic defects such as voids or inclusions. At magnifications of 1,000× and 2,000×, the surface texture became more pronounced, revealing features mainly in the 1–2 μm size range. These features are likely due to the polymer composition, which can lead to slight variations in surface texture that arise during processing. The even distribution of these features suggests deliberate material processing, resulting in a homogenous surface that increases its mechanical durability.

When magnified up to 5,000×, the microstructure of the material became more discernible (see Fig. 6, *c*). The *SEM* images revealed a smooth and homogenous texture without any visible crystalline formations,

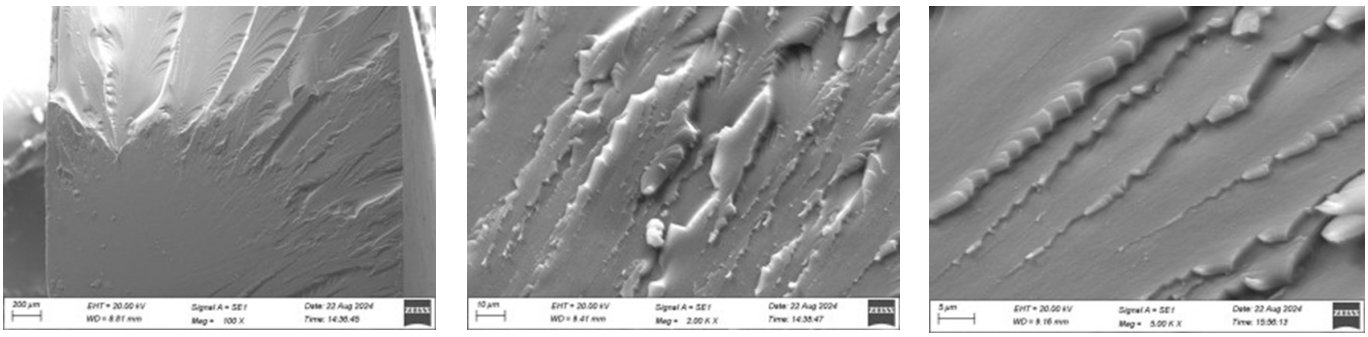

a *b* *c*

Fig. 6. SEM images for base Acrylate material at different magnification:
a – 100× magnification, 200 μm; *b* – 2,000× magnification, 10 μm; *c* – 5,000× magnification; 5 μm

indicating a predominantly amorphous structure of the base material. The absence of observable crystalline domains suggests that the material is specifically designed for applications requiring flexibility and impact resistance, which are often associated with amorphous polymers.

EDS Analysis and Elemental Composition

The results of *EDS* analysis for the base Acrylate material are presented in Figs. 7, *a* and 7, *b*. The *EDS* investigation enabled quantitative determination of the elemental composition of the base material, revealing that it primarily consists of carbon (*C*) and oxygen (*O*). In one region, the elemental composition was determined to be approximately 71.17 wt. % carbon and approximately 28.83 wt .% oxygen; in another region, approximately 72.21 wt. % carbon and approximately 27.79 wt. % oxygen. The composition of substances was determined as 76.68 wt. % carbon and 23.32 wt. % oxygen, and 77.59 wt. % carbon and 22.41 wt. % oxygen, respectively.

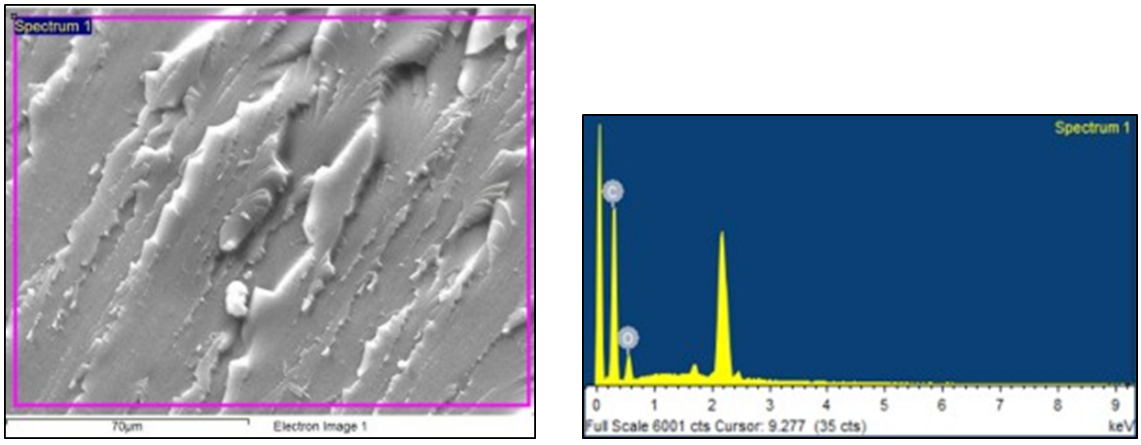

a *b*

Fig. 7. EDS analysis for base Acrylate material:
a – spectrum with 70 μm; *b* – *EDS* graph for 70 μm Spectrum

The high carbon content is a characteristic feature of polymer materials, in which carbon plays the role of the primary structural element, as also shown in Fig. 7, *b*. The detected oxygen is likely associated with the presence of functional groups such as carbonyl (*C=O*) or ether (*C-O-C*) groups, which are characteristic of polymers, such as *PEEK* (polyetheretherketone). These groups contribute to enhanced thermal stability and chemical resistance of the material, improving its performance characteristics in demanding applications.

Characterisation of 5 % wt. PEEK Material in Acrylate

Surface Morphology and Microstructural Features

SEM images of 5 % wt. *PEEK* material in Acrylate, acquired at various magnifications, are presented in Figs. 8, *a*, *b*, and *c*. Analysis of the composite material using scanning electron microscopy was performed to investigate its surface morphology and microstructure. Magnifications ranging from 500× to 5,000× at an accelerating voltage of 20 kV were used. This range enabled a comprehensive evaluation of both general surface characteristics and microstructural features and provided valuable information regarding the effect of *PEEK* addition to the underlying polymer matrix (Fig. 8, *a*).

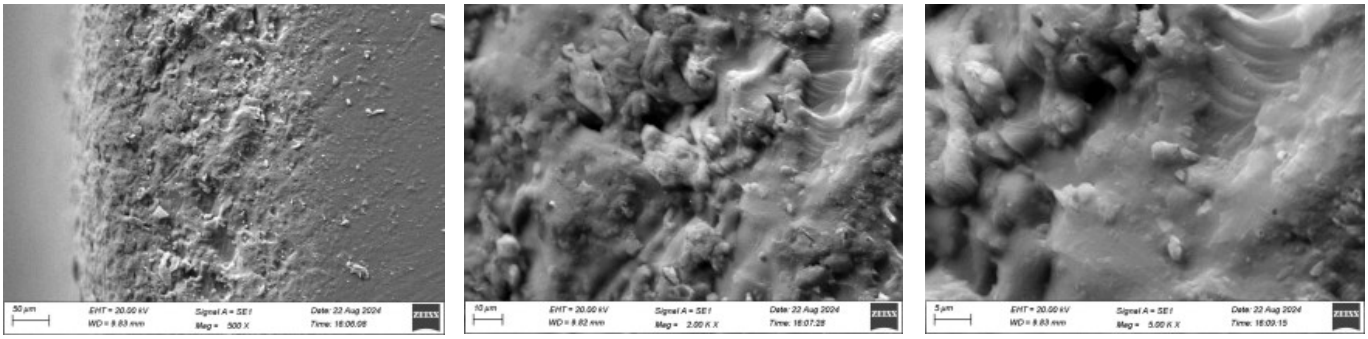

a *b* *c*

Fig. 8. SEM images for 5 wt. % *PEEK* in Acrylate material at different magnification:
a – 500× magnification, 50 μm; *b* – 2,000× magnification, 10 μm; *c* – 5,000× magnification, 5 μm

At 500× magnification, the SEM images exhibit a relatively smooth and homogenous surface with minimal deviations, comparable to those of the base material. However, the addition of *PEEK* resulted in slight changes in the surface texture. These changes are likely due to the dispersion of *PEEK* within the polymer matrix.

A more detailed investigation of the material's microstructure was conducted at magnifications of 1,000× and 2,000×. The *PEEK* particles are visible as separate and relatively evenly distributed phases within the matrix. Their sizes are in the micron range, ranging from 1 to 2 μm. The observed distribution indicates effective *PEEK* incorporation into the matrix, contributing to the composite's homogeneity.

At a maximum magnification of 5,000×, images were obtained that demonstrate a more detailed view of the *PEEK* distribution. The *PEEK* particles are characterized by excellent dispersion and seamless integration into the polymer matrix without noticeable signs of aggregation.

The addition of *PEEK* does not disrupt the predominantly amorphous structure of the material, which is important for maintaining its natural flexibility and toughness. Overall, the surface retains an amorphous appearance.

EDS Analysis and elemental composition

Energy dispersive spectroscopy (*EDS*) examination of the 5 wt. % polyetheretherketone (*PEEK*) in Acrylate revealed that its elemental composition is predominantly carbon (*C*) and oxygen (*O*), consistent with the composition of the base Acrylate material (Fig. 9).

Table 3 presents the data on the composition of 5 % wt. *PEEK* in Acrylate composites material. The mass percentage of carbon was approximately 70.75 %, while that of oxygen was 29.25 %. The atomic proportions of the elements are 76.32% for carbon and 23.68% for oxygen. These results indicate a similarity in the elemental composition between the base Acrylate material and the *PEEK* composite, suggesting a negligible influence of *PEEK* addition on the overall elemental composition. The slight increase in oxygen content is attributed to the presence of oxygen-rich functional groups in *PEEK* (such as ether and carbonyl groups), which are uniformly distributed within the polymeric matrix.

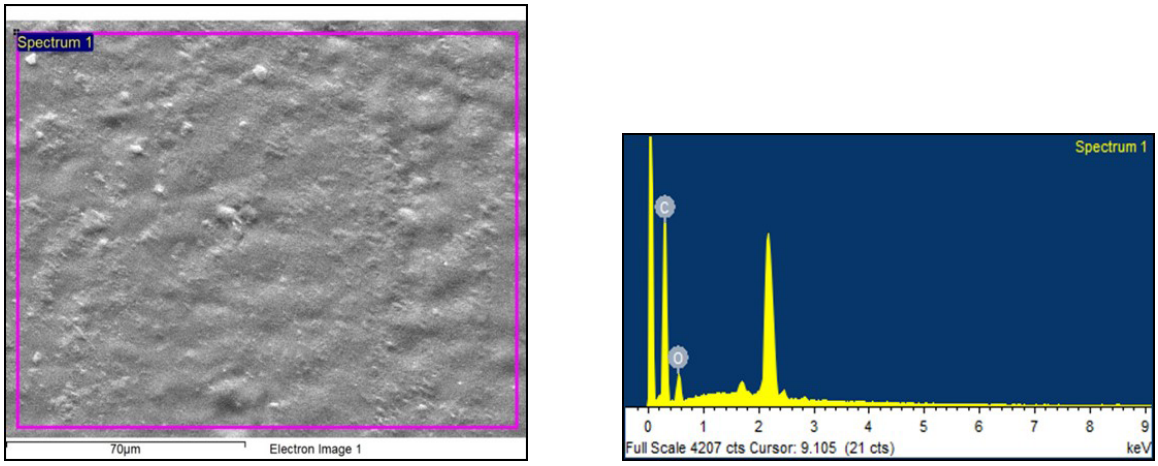

a *b*

Fig. 9. EDS analysis for 5 wt. % *PEEK* in Acrylate material:
a – spectrum with 70 µm; *b* – *EDS* graph for 70 µm spectrum

Table 3

Composition of 5 % wt. *PEEK* in Acrylate composites material

Element	Weight (%)	Atomic (%)
C	70.75	76.32
O	29.25	23.68
Totals	100.00	–

As evidenced by the *SEM* images, the incorporation of 5 wt. % *PEEK* into the polymeric matrix leads to the formation of characteristic microstructural features. The uniform distribution of the *PEEK* particles within the matrix contributes to enhanced mechanical properties of the material, such as stiffness and strength, through reinforcement of the polymer structure. Despite the *PEEK* addition, the composite retains a predominantly amorphous structure, which is favorable for maintaining important characteristics such as impact toughness. The *EDS* data confirm that the elemental composition of the composite largely remains unchanged, with carbon and oxygen being predominant. The slight increase in oxygen concentration indicates successful *PEEK* integration into the matrix, suggesting the absence of significant phase separation and inhomogenuity.

Characterization of 10 % wt. PEEK Material in Acrylate

Surface Morphology and Microstructural Features

The morphology and microstructure of a composite material containing 10 wt. % *PEEK* were investigated using scanning electron microscopy (*SEM*) at magnifications ranging from 500× to 5,000× and an accelerating voltage of 20 kV (Fig. 10, *a*, *b*, *c*).

This approach enabled a detailed examination of the material's surface morphology and microstructure, as well as an evaluation of the impact of the increased *PEEK* content on its structure.

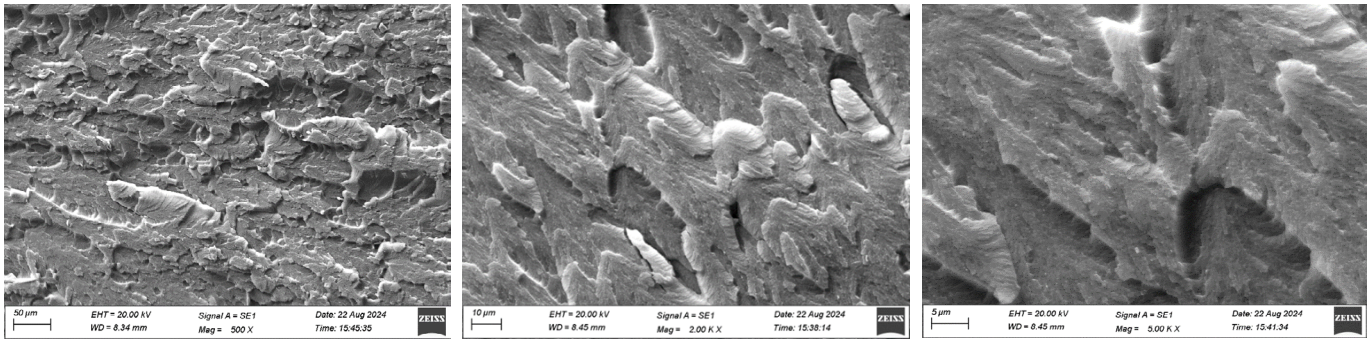

a *b* *c*

Fig. 10. SEM images for 10 wt. % *PEEK* in Acrylate material at different magnification:
a – 500× magnification, 50 µm; *b* – 2,000× magnification, 10 µm; *c* – 5,000× magnification, 5 µm

At 500× magnification, the material's surface exhibited a relatively smooth texture, comparable to materials containing a lower concentration of *PEEK*. However, the higher *PEEK* concentration led to more pronounced differences in the texture, indicating a significant influence of the *PEEK* particles on the surface composition. The observed changes were subtle but consistent, suggesting a uniform distribution of *PEEK* within the matrix (Fig. 10, *b*).

Increasing the magnification to 2000× made the *PEEK* particles more visibile. They were observed as discrete inclusions within the polymer matrix, with a size of approximately 1–2 µm. The distribution pattern indicates good integration of *PEEK* into the base material, promoting enhanced structural homogeneity and, consequently, improved mechanical properties of the composite.

At 5,000× magnification (Fig. 10, *c*), the *SEM* images provided more detailed information about the microstructural features, confirming the uniform distribution of *PEEK* particles and the absence of aggregation. The surface maintained an amorphous structure, with the presence of *PEEK* contributing to minor variations in texture that did not disrupt the overall smoothness of the material. This homogeneous component distribution is critical for achieving an optimal balance of flexibility and strength, which is necessary for the intended application of this material.

EDS Analysis and elemental composition

EDS analysis provided precise and quantitative data regarding the elemental composition of the 10 wt. % *PEEK* material. The primary elements identified were carbon (*C*) and oxygen (*O*), consistent with the composition of *PEEK* and the base polymer (Fig. 11).

Table 4 presents the elemental composition of 10 wt. % *PEEK* in Acrylate. The substance in a specific area consisted of approximately 70.19 wt. % carbon and 29.81 wt. % oxygen. In other locations, additional

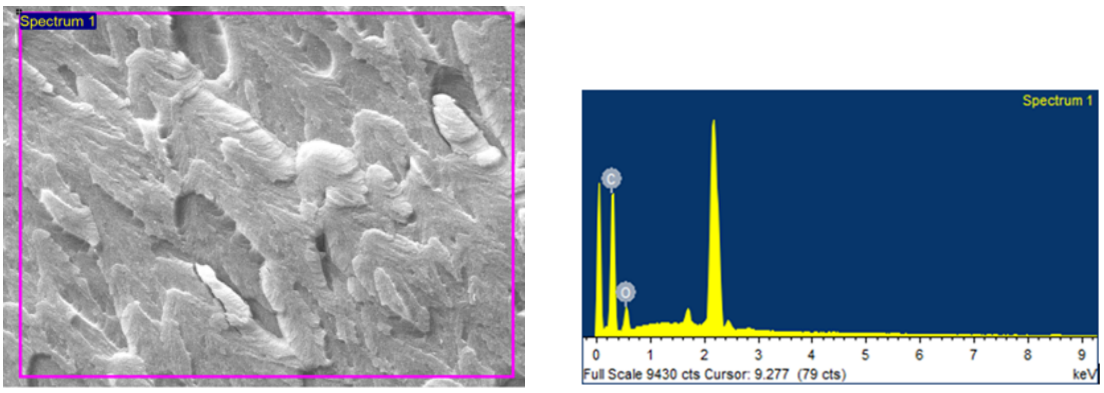

a *b*

Fig. 11. EDS analysis for 10 wt. % *PEEK* in Acrylate material:
a – spectrum with 70 µm; *b* – *EDS* graph for 70 µm spectrum

Table 4

Composition of 10 % wt. *PEEK* in Acrylate composites material

Element	Weight (%)	Atomic (%)
C	70.19	75.82
O	29.81	24.18
Totals	100.00	–

elements, such as gold (*Au*), were observed, which were applied onto the surface to improve image contrast. The elemental distribution confirms that the presence of *PEEK* does not significantly affect the base composition, but introduces functional groups associated with the chemical structure of *PEEK*. Fluctuations in oxygen levels in different locations may be related to the presence of these functional groups, which are important for *PEEK* properties, including its thermal stability and resistance to harsh environments. The data from scanning electron microscopy (*SEM*) and energy-dispersive X-ray spectroscopy (EDS) collectively show that the addition of 10 wt. % *PEEK* to the base material has a significant impact on the microstructure, especially compared to lower *PEEK* concentrations.

SEM images show a uniform distribution of *PEEK* particles, which, in turn, leads to an increase in mechanical properties such as stiffness and tensile strength. This improvement in mechanical properties can be explained by the reinforcing action of the particles within the polymer matrix. The inherent amorphous structure of the material, which is maintained even at the higher *PEEK* concentration, is advantageous for maintaining its flexibility and impact toughness. *EDS* analysis confirms these findings, demonstrating that the composition of the material mainly corresponds to the composition of *PEEK*, with carbon and oxygen being the main components. The inclusion of *PEEK* particles does not lead to significant phase separation, thereby maintaining a homogeneous structure in the composite.

Discussion: The incorporation of *PEEK* into the Acrylate polymer matrix at concentrations of 5 wt. % or 10 wt. % enhances the mechanical properties of the material by reinforcing the structure, while the material maintains flexibility and surface smoothness. These composites possess a balanced combination of strength, durability, and adaptability, making them optimal candidates for applications where these characteristics are essential. The choice between 5 wt. % and 10 wt. % *PEEK* content will depend on the specific mechanical property requirements of the material based on the intended application, where higher *PEEK* concentrations will provide increased stiffness and strength.

Wear testing results

The results of pin-on-disc wear tests conducted on samples of base Acrylate, a 5 wt. % *PEEK* in Acrylate composite, and a 10 wt. % *PEEK* in Acrylate composite clearly demonstrate the impact of *PEEK* reinforcement on the wear resistance and frictional properties of Acrylate.

Table 5 presents the experimental observations obtained during the pin-on-disc wear tests. A systematic analysis of friction coefficients, wear rates, and *SEM* images of the worn surfaces clearly shows the benefits of *PEEK* reinforcement for improving the tribological properties in applications where the material is subjected to loads.

The wear test results demonstrate a pronounced relationship between the degree of reinforcement, wear resistance, and frictional characteristics for the base Acrylate, a 5 wt. % *PEEK* in Acrylate composite, and a 10 wt. % *PEEK* in Acrylate composite. The base Acrylate exhibited a friction coefficient of 0.45 and the highest wear rate, measured at 1.2×10^{-6} $mm^3/N\cdot m$.

SEM analysis of the base Acrylate surface revealed visible wear tracks and significant material removal, indicating its limited wear resistance, which is expected for an unreinforced polymer. The friction coefficient for the 5 wt. % *PEEK* in Acrylate composite decreased to 0.40, and the wear rate decreased to 0.9×10^{-6} $mm^3/N\cdot m$. *SEM* images of the 5 wt. % *PEEK* composite surface showed improved uniformity and moderate wear tracks, indicating that the introduction of 5 wt. % reinforcing particles enhances the material's structural integrity and, consequently, its wear resistance.

Table 5

Experimental Observation Table for Pin-on-Disk Wear Test

Material Type	Normal Load (N)	Sliding Speed (m/s)	Sliding Distance (m)	Wear Rate ($mm^3/N{\cdot}m$)	Coefficient of Friction	SEM observations
Base Acrylate	10	1	1,000	1.2×10^{-6}	0.45	Smooth surface with slight wear tracks; minor material removal observed
5 % wt. *PEEK* in Acrylate composites	10	1	1,000	0.9×10^{-6}	0.4	Increased uniformity: moderate wear marks but reduced material loss compared to base Acrylate
10 % wt. *PEEK* in Acrylate composites	10	1	1,000	0.7×10^{-6}	0.35	Enhanced surface homogeneity; minimal wear tracks, indicating higher wear resistance

The 10 wt. % *PEEK* in Acrylate composite demonstrated the best wear resistance among the tested materials, with a wear rate of $0.7{\times}10^{-6}$ $mm^3/N{\cdot}m$ and a friction coefficient of 0.35. *SEM* images of the 10 wt. % *PEEK* in Acrylate composite surface revealed high uniformity and minimal wear tracks, indicating a significant improvement in wear resistance at this reinforcing component concentration. This improvement is likely due to the uniform distribution of reinforcing particles, which effectively prevents material degradation under friction and load.

Increasing the degree of reinforcement from base Acrylate to the 10 wt. % *PEEK* composite leads to an improvement in both wear resistance and frictional properties. This indicates that increasing the degree of reinforcement enhances the structural integrity of the composite, reducing erosion and friction under high-load conditions. Fig. 12 shows a liner fabricated via *DLP* 3D-printing from the 10 wt. % *PEEK* in Acrylate composite biomaterial. This allows for the conclusion that the 10 wt. % *PEEK* in Acrylate biomaterial is suitable for 3D-printing at room temperature in order to obtain the desired geometry for orthopedic implants.

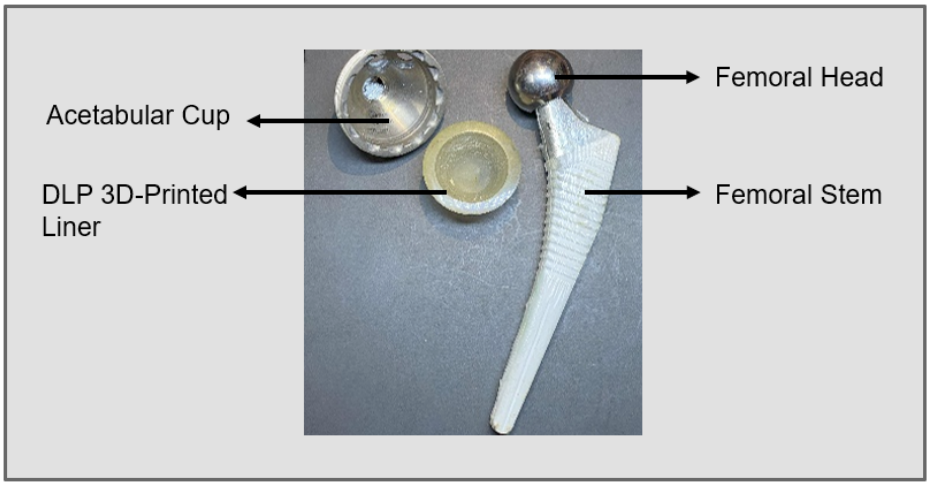

Fig. 12. DLP 3D-printed hip joint implant liner made from Acrylate composite with 10 wt % *PEEK*

Conclusion

This study highlights the advanced properties of 10 wt. % *PEEK* in Acrylate composites biomaterials, demonstrating their enhanced wear resistance and improved mechanical properties compared to Acrylate composites with lower *PEEK* content and base Acrylate materials.

– The 10 wt. % *PEEK* in Acrylate composites biomaterial possesses an optimal balance of strength, stiffness, and ductility, which is critical for load-bearing applications such as orthopedic implants. Pin-on-disc wear tests showed a significant reduction in the specific wear rate of the 10 wt. % *PEEK* in Acrylate composite at various loads and speeds, confirming its suitability for use in high-stress environments.

– *SEM* and *EDS* studies confirmed the uniform distribution of *PEEK* particles within the polymer matrix, which ensures improved mechanical properties and durability of the composite material.

– The ability of the 10 wt. % *PEEK* in Acrylate composite to maintain mechanical integrity under harsh tribological conditions makes it a promising material for long-term applications in orthopedics, particularly in joint implants where wear resistance and mechanical characteristics are crucial for successful implantation.

– The improved wear resistance and enhanced mechanical strength of this composite reduce the risk of implant failure due to material degradation, which is an important factor determining the lifespan of hip-joint implants.

– The 10 wt. % *PEEK* in Acrylate composite biomaterial can be processed using *DLP* 3D-printing at room temperature, and the resulting products are suitable for the fabrication of biomedical implants, prosthetic implants, tissue engineering scaffolds, and other healthcare applications.

However, further research is needed to fully understand the behavior of these composite materials in realistic clinical conditions.

– Future studies should focus on fatigue testing to evaluate the material's durability under cyclic loading conditions that simulate the loads experienced by implants installed within the human body.

– In addition, clinical trials are needed to confirm the biocompatibility and performance of this material over extended periods.

References

1. Ahmad J.R., Aldo F.M., Ifran S., Tri K., Yudan W. The needs of current implant technology in orthopaedic prosthesis biomaterials application to reduce prosthesis failure rate. *Journal of Nanomaterials*, 2016, art. 5386924. DOI: 10.1155/2016/5386924.

2. Garcia E., Fernandez A., Martin L. Comparative analysis of traditional and advanced materials for hip joint implants. *Materials Science and Engineering C*, 2020, vol. 112, p. 110857. DOI: 10.1080/17453674.2018.1427320.

3. Verma S., Sharma N., Kango S., Sharma S. Developments of PEEK (Polyetheretherketone) as a biomedical material: a focused review. *European Polymer Journal*, 2021, vol. 147, p. 110295. DOI: 10.1016/j.eurpolymj.2021.110295.

4. Luo C., Liu Y., Peng B., Chen M., Liu Z., Li Z., Kuang H., Gong B., Li Z., Sun H. PEEK for oral applications: recent advances in mechanical and adhesive properties. *Polymers*, 2023, vol. 15 (2). DOI: 10.3390/polym15020386.

5. Obinna O., Stachurek I., Kandasubramanian B., Njuguna J. 3D printing for hip implant applications: a review. *Polymers*, 2020, vol. 12 (11), p. 2682. DOI: 10.3390/polym12112682.

6. Dama Y., Jogi B., Pawade R., Kulkarni A. Impact of print orientation on wear behavior in FDM printed PLA biomaterial: study for hip-joint implant. *Obrabotka metallov (tekhnologiya, oborudovanie, instrumenty) = Metal Working and Material Science*, 2024, vol. 26, no. 4, pp. 19–40. DOI: 10.17212/1994-6309-2024-26.4-19-40.

7. Xue Z., Wang Z., Sun A., Huang J., Wu W., Chen M., Hao X., Huang Z., Lin X., Wenig S. Rapid construction of polyetheretherketone (PEEK) biological implants incorporated with brushite ($CaHPO_4 \cdot 2H_2O$) and antibiotics for anti-infection and enhanced osseointegration. *Materials Science & Engineering: C*, 2020, vol. 111, p. 110782. DOI: 10.1016/j.msec.2020.110782.

8. Zhang X., Zhang T., Chen K., Xu H., Feng C., Zhang D. Wear mechanism and debris analysis of PEEK as an alternative to CoCrMo in the femoral component of total knee replacement. *Friction*, 2023, vol. 11 (10), pp. 1845–1861. DOI: 10.1007/s40544-022-0700-z.

9. Cassari L., Zamuner A., Messina G.M.L., Marsotto M., Chen H., Gonnella G., Coward T., Battocchio C., Huang J., Iucci G., Marletta G., Di Silvio L., Dettin M. Bioactive PEEK: surface enrichment of vitronectin-derived adhesive peptides. *Biomolecules*, 2023, vol. 13 (2), p. 246. DOI: 10.3390/biom13020246.

10. Yu D., Lei X., Zhu H. Modification of polyetheretherketone (PEEK) physical features to improve osteointegration. *Journal of Zhejiang University-Science B*, 2022, vol. 23 (3), pp. 189–203. DOI: 10.1631/jzus.B2100622.

11. Du X., Ronayne S., Lee S.S., Hendry J., Hoxworth D., Bock R., Ferguson S.J. 3D-printed PEEK/silicon nitride scaffolds with a triply periodic minimal surface structure for spinal fusion implants. *ACS Applied Bio Materials*, 2023, vol. 6 (8), pp. 3319–3329. DOI: 10.1021/acsabm.3c00383.

12. Han X., Sharma N., Spintzyk S., Zhou Y., Xu Z., Thieringer F.M., Rupp F. Tailoring the biologic responses of 3D printed PEEK medical implants by plasma functionalization. *Dental Materials*, 2022, vol. 38 (7), pp. 1083–1098. DOI: 10.1016/j.dental.2022.04.026.

13. Dama Y.B., Jogi B.F., Pawade R.S. Application of nonlinear analysis in evaluating additive manufacturing processes for engineering design features: a study and recommendations. *Communications on Applied Nonlinear Analysis*, 2024, vol. 31 (1s). DOI: 10.52783/cana.v31.559.

14. Kharate N., Anerao P., Kulkarni A., Abdullah M. Explainable AI techniques for comprehensive analysis of the relationship between process parameters and material properties in FDM-based 3D-printed biocomposites. *Journal of Manufacturing and Materials Processing*, 2024, vol. 8 (4), p. 171. DOI: 10.3390/jmmp8040171.

15. Reddy K.U.K., Verma P.C., Rathi A., Saravanan P. A comprehensive mechanical characterization of as-printed and saliva soaked 3D printed PEEK specimens for low-cost dental implant applications. *Materials Today Communications*, 2023, vol. 36, p. 106438. DOI: 10.1016/j.mtcomm.2023.106438.

16. Zhang W., Yuan Z., Meng X., Zhang J., Long T., Yaochao Z., Yang C., Lin R., Yue B., Guo Q. Wang Y. Preclinical evaluation of a mini-arthroplasty implant based on polyetheretherketone and Ti6AI4V for treatment of a focal osteochondral defect in the femoral head of the hip. *Biomedical Materials*, 2020, vol. 15 (5), p. 055027. DOI: 10.1088/1748-605x/ab998a.

17. Du X., Ronayne S., Lee S.S., Hendry J., Hoxworth D., Bock R., Ferguson S.J. 3D-printed PEEK/silicon nitride scaffolds with a triply periodic minimal surface structure for spinal fusion implants. *ACS Applied Bio Materials*, 2023, vol. 6 (8), pp. 3319–3329. DOI: 10.1021/acsabm.3c00383.

18. Lim K.M., Park T.H., Lee S.J., Park S.J. Design and biomechanical verification of additive manufactured composite spinal cage composed of porous titanium cover and PEEK body. *Applied Sciences*, 2019, vol. 9 (20), p. 4258. DOI: 10.3390/app9204258.

19. Gosavi A., Kulkarni A., Dama Y., Deshpande A., Jogi B. Comparative analysis of drop impact resistance for different polymer-based materials used for hearing aid casing. *Materials Today: Proceedings*, 2022, vol. 49, pp. 2433–2441. DOI: 10.1016/j.matpr.2021.09.519.

20. Carpenter R.D., Klosterhoff B.S., Torstrick F.B., Foley K.T., Burkus J.K., Lee C.S., Gall K., Guldberg R.E., Safranski D.L. Effect of porous orthopaedic implant material and structure on load sharing with simulated bone ingrowth: a finite element analysis comparing titanium and PEEK. *Journal of the Mechanical Behavior of Biomedical Materials*, 2018, vol. 80, pp. 68–76. DOI: 10.1016/j.jmbbm.2018.01.017.

21. Virpe K., Deshpande A., Kulkarni A. A review on tribological behavior of polymer composite impregnated with carbon fillers. *AIP Conference Proceedings*, 2020, vol. 2311 (1). DOI: 10.1063/5.0035408.

22. Paturkar A., Mache A., Deshpande A., Kulkarni A. Experimental investigation of dry sliding wear behavior of jute/epoxy and jute/glass/epoxy hybrids using Taguchi approach. *Materials Today: Proceedings*, 2018, vol. 5 (11), pp. 23974–23983. DOI: 10.1016/j.matpr.2018.10.190.

23. Satkar A.R., Mache A., Kulkarni A. Numerical investigation on perforation resistance of glass-carbon/epoxy hybrid composite laminate under ballistic impact. *Materials Today: Proceedings*, 2022, vol. 59 (1), pp. 734–741. DOI: 10.1016/j.matpr.2021.12.464.

24. Chinchanikar S. Modeling of sliding wear characteristics of Polytetrafluoroethylene (PTFE) composite reinforced with carbon fiber against SS304. *Obrabotka metallov (tekhnologiya, oborudovanie, instrumenty) = Metal Working and Material Science*, 2022, vol. 24, no. 3, pp. 40–52. DOI: 10.17212/1994-6309-2022-24.3-40-52.

25. Kanitkar Y.M., Kulkarni A.P., Wangikar K.S. Investigation of flexural properties of glass-Kevlar hybrid composite. *European Journal of Engineering and Technology Research*, 2018, vol. 1 (1), pp. 25–29. DOI: 10.24018/ejeng.2016.1.1.90.

26. Pal S., Gaikwad Y., Asha S.K. Room temperature photocurable PEEK polymer formulations for high-performance 3D printing applications. *ACS Applied Engineering Materials*, 2024, vol. 2 (6), pp. 1450–1459. DOI: 10.1021/acsaenm.4c00275.

27. Anerao P., Kulkarni A., Munde Y., Shinde A., Das O. Biochar-reinforced PLA composite for fused deposition modeling (FDM): a parametric study on mechanical performance. *Composites Part C: Open Access*, 2023, vol. 12, p. 100406. DOI: 10.1016/j.jcomc.2023.100406.

28. Devane P.A., Horne J.G., Martin K., Coldham G., Krause B. Three-dimensional polyethylene wear of a press-fit titanium prosthesis. *The Journal of Arthroplasty*, 1997, vol. 12 (3). DOI: 10.1016/S0883-5403(97)90021-8.

Conflicts of Interest

The authors declare no conflict of interest.